CHAPTER 2:

Some Theoretical Understanding of Brillouin Fiber Laser and Important Parameters for Measurements

2.1 Maxwell's Equations and Electromagnetic Wave Propagation in Linear and Nonlinear Medium

The macroscopic description of the interaction of light fields with a medium containing no magnetization and no current due to free charges will be briefly discussed using Maxwell's equations. For the first time, a unified treatment of electric and magnetic fields was developed by Maxwell in the 1860s. It is necessary to consider the electromagnetic wave propagation in a nonlinear medium for understanding the nonlinear phenomena in an optical fiber. Here, we are going to describe the general Maxwell equations that govern the electromagnetic wave propagation in an SMF. Maxwell's equations are expressed below in MKS units

$$\nabla \cdot \mathbf{D} = \rho_v \tag{2.1}$$

$$\nabla \cdot \mathbf{B} = 0 \tag{2.2}$$

$$\nabla \times \mathbf{E} = -\frac{\partial \mathbf{B}}{\partial t} \tag{2.3}$$

$$\nabla \times \mathbf{H} = \mathbf{J} + \frac{\partial \mathbf{D}}{\partial t} \tag{2.4}$$

where, **E** and **H** are the electric and magnetic intensity fields, and **B** and **D** are the electric and magnetic induction fields. The volume density of the free charge ρ_v and the current density **J** are connected together by the law of charge conservation

$$\nabla \bullet \mathbf{J} + \frac{\partial \rho_v}{\partial t} = 0 \tag{2.5}$$

It us imperative to note that these two values are both zero throughout this work because our attention will be confined exclusively to no magnetization insulating materials, rather than metals or doped semiconductors, discussed by Shen [1]. From Maxwell's equations, it is evident that the tangential component of **E** and **H**, and the normal components of **D** and **B** are continuous at the boundary interfaces that separate distinct media. The fields are related through constitutive relations

$$\mathbf{D} = \varepsilon \mathbf{E} = \varepsilon_0 \mathbf{E} + \mathbf{P} \tag{2.6}$$

$$\mathbf{B} = \mu \mathbf{H} + \mathbf{M} \tag{2.7}$$

where **P** and **M** are the electric dipole moment per unit volume or electric polarization, and magnetic moment per unit volume or magnetization, respectively. As said before, we shall confine our attention to nonmagnetic media, where $\mathbf{M} \equiv 0$ and neglect higher order multipoles. μ and ε are the permeability and the permittivity of the medium and ε_0 is the vacuum permittivity. In the optical frequency range, μ can be replaced by $(\varepsilon_0 c^2)^{-1}$, where c is the speed of light in a vacuum. Using Maxwell's equations, Eqs. (2.3) and (2.4), in addition to Eq. (2.6), one can obtain the fundamental equation for the propagation of an electric field in both linear and nonlinear medium as

$$\nabla\times(\nabla\times\mathbf{E}) - \frac{1}{c^2}\frac{\partial^2\mathbf{E}}{\partial t^2} = \frac{1}{\varepsilon_0 c^2}\frac{\partial^2\mathbf{P}}{\partial t^2} \tag{2.8}$$

where in Cartesian coordinates, we have the following:

$$\nabla\times(\nabla\times\mathbf{E}) = \nabla^2\mathbf{E} - \nabla(\nabla\cdot\mathbf{E}) \tag{2.9}$$

Eq. (2.8) will be the central equation for describing the propagation of the electric field in linear and nonlinear media. In order to make any use of it, we must somehow specify the polarization **P**. This cannot be done only within the Maxwell equations since **P** is a property of the material medium that the field **E** propagates in. To proceed, we need to know how a dipole moment density **P** is produced in the medium. In other words, we require information on the relationship between **P** and **E** which will be discussed later. However, in linear media, **P** and **E** are related by the electric susceptibility function χ as

$$\mathbf{P} = \varepsilon_0\chi\mathbf{E} \tag{2.10}$$

where χ is a constant. Then Eq. (2.8) becomes

$$\nabla^2\mathbf{E} - \frac{1}{v^2}\frac{\partial^2\mathbf{E}}{\partial t^2} = 0 \tag{2.11}$$

which is the wave equation for the electric field in a linear medium and $v = \frac{c}{n}$ is the wave velocity of the electric field propagation in the medium with the refractive index $n=\sqrt{1+\chi}$. A similar procedure applied to the magnetic field instead results in the wave equation for the magnetic field in a linear medium as

$$\nabla^2\mathbf{H} - \frac{1}{v^2}\frac{\partial^2\mathbf{H}}{\partial t^2} = 0 \qquad (2.12)$$

The solutions of Eqs. (2.11) and (2.12) are in the form of propagating functions especially the time-harmonic case such as

$$\mathbf{E} = \mathbf{E}_0 \cos(\omega t \pm \beta z) \qquad (2.13)$$

where ω is the radian frequency and β, known as the wave propagation constant is the phase shift per unit distance of the wave measured along the z axis. For a uniform plane wave, we have $\beta = \frac{\omega}{v}$. In the real instantaneous form, the electric field (and also magnetic field) propagating in a lossless medium can be expressed as

$$\mathbf{E} = \frac{1}{2}\mathbf{E}_0 \{ \exp(i(\omega t \pm \beta z + \Phi)) + \text{c.c.} \} \qquad (2.14)$$

where E_0 is magnitude and direction of the electric field, Φ represents an overall phase, and c.c. denotes the complex conjugate of the preceding term. Such a wave is an example of a uniform plane wave in which the electric and magnetic fields lying in the plane transverse to the propagation of direction (z-axis) have no variation in any other direction within the transverse plane. The propagating fields transport energy. According to Poynting's theorem:

$$\mathbf{S} = \mathbf{E} \times \mathbf{H} \qquad (2.15)$$

where **S** is referred to as Poynting's vector is the flow of the transported power associated with the fields, per unit cross-sectional area. It can be shown that the second conservation law is with the Poynting's vector

$$\nabla \cdot \mathbf{S} = \frac{\partial u}{\partial t} + W \qquad (2.16)$$

where $u = \frac{1}{2}(\mathbf{E}\cdot\mathbf{D} + \mathbf{B}\cdot\mathbf{H})$ is the internal energy per unit volume, and $W = \mathbf{E}\cdot\mathbf{J}$,the power dissipation per unit volume in the system, is zero in our work in which there is no current. The fields are the real instantaneous forms leading to the instantaneous power density. However, in practice the time-average power is usually measured due to the fast oscillating fields. Therefore, most detection equipments such as a power meter can not respond fast enough to follow the oscillating fields at high frequencies, so they effectively integrate the instantaneous power.

$$\prec \mathbf{S} \succ = \frac{1}{T}\int_0^T (\mathbf{E}\times\mathbf{H})\, dt \qquad (2.17)$$

in which $T = \frac{2\pi}{\omega}$ is the oscillation period.

2.2 Field Analysis of the Step Index Fiber as a Linear Medium

Considering a single mode step index fiber oriented along the z axis, the effect of the fiber is to restrict the propagating electromagnetic fields in the transverse plane (x-y) so that derivatives of the fields with respect to the transverse components will be nonzero. Due to the cylindrical symmetry of the optical fiber, the electric field can be written as $\mathbf{E} = \mathbf{E_0}(r,\varphi)\, e^{i(\omega t-\beta z)}$ where β is the propagation constant and in the case of the uniform plane wave, $\beta = \frac{\omega}{v}$. According to Maxwell's equations, out of the six components of **E** and **H**, only two components are independent and the others can be expressed in terms of these two. It is common to choose E_z and H_z as the two independent components. Then due to the cylindrical symmetry of optical fibers, the wave equation (2.11) for the electric field $E(r, \varphi, z)$ is expressed in cylindrical coordinates as:

$$\nabla^2 \mathbf{E}_z + n^2 k_0^2 \mathbf{E}_z = \frac{\partial^2 \mathbf{E}_z}{\partial r^2} + \frac{1}{r}\frac{\partial \mathbf{E}_z}{\partial r} + \frac{1}{r^2}\frac{\partial^2 \mathbf{E}_z}{\partial \varphi^2} + \frac{\partial^2 \mathbf{E}_z}{\partial z^2} + n^2 k_0^2 \mathbf{E}_z = \mathbf{0} \tag{2.18}$$

in which $k_o = \frac{\omega}{c}$ and $n = \frac{c}{\mathrm{v}}$ is the refractive index of the medium. Although Eq. (2.11) is valid in a linear medium where **P** and **E** are related by Eq. (2.6), it is useful in the treatment of the small perturbation approximation in nonlinear medium because nonlinear effects are relatively weak especially in silica fibers. Using the method of separation of variables, E_z = R(r) $\phi(\varphi)$, the wave equation can be easily solved, first by defining $k^2 = n^2 k_0^2 - \beta^2$,

$$r^2 \phi \frac{\partial^2 \mathrm{R}}{\partial r^2} + r\phi \frac{\partial \mathrm{R}}{\partial r} + \mathrm{R}\frac{\partial^2 \phi}{\partial \varphi^2} + k^2 r^2 \mathrm{R}\phi = 0 \tag{2.19}$$

Dividing Eq. (2.19) by R(r) $\phi(\varphi)$, we have

$$\frac{r^2}{R}\frac{d^2 R}{dr^2} + \frac{r}{R}\frac{dR}{dr} + k^2 r^2 = -\frac{1}{\phi}\frac{d^2 \phi}{d\varphi^2} \tag{2.20}$$

The left-hand side of Eq. (2.20) depends only on r, whereas the right-hand side depends only on φ. Since r and φ are independent variable, it must follow that each side of Eq. (2.20) must be equal to a constant. Supposing this constant to be m^2, Eq. (2.20) separate into the following two equations:

$$\frac{1}{\phi}\frac{d^2 \phi}{d\varphi^2} = -m^2 \tag{2.21}$$

$$\frac{d^2 R}{dr^2} + \frac{1}{r}\frac{dR}{dr} + (k^2 - \frac{m^2}{r^2})R = 0 \tag{2.22}$$

Solving Eq. (2.21) results in

$$\phi(\varphi) = A\cos(m\varphi + \alpha) + B\sin(m\varphi + \alpha) \tag{2.23}$$

m is an integer since it is needed that the field be self-consistent on each rotation of φ through 2π. A, B, and α are constants and their values depend on the boundary conditions. Eq. (2.22) is a form of Bessel's equations so that its solution is in terms of Bessel function of the order m. Since this equation is a second order differential equation, it has two linear independent solutions, the Bessel function of the first kind $J_m(kr)$ and the second kind Neumann $N_m(kr)$ which apply to cases of real integer m. However, if m is imaginary, the solution will consist of the first and second modified Bessel functions, K_m and I_m, respectively.

$$R(r) = \begin{cases} A_1 J_m(kr) + A_2 N_m(kr) & real\ \ k \\ B_1 K_m(|k|r) + B_2 I_m(|k|r) & imaginary\ \ k \end{cases} \tag{2.24}$$

The solution must satisfy two boundary conditions. (1) The solution in the core must be oscillatory without any singularities. (2) The solution in the cladding must monotonically decreases as the radius increases to satisfy the boundary conditions on the fiber. The first condition suggests the ordinary Bessel functions in the core region $(r \le a)$ so that $k = (n_1^2 k_0^2 - \beta^2)^{\frac{1}{2}} = k_1$ must be real in this region with the refractive index n_1. On the other hand, we have to choose $A_2 = 0$ since Neumann functions $N_m(kr)$ have singularities at $r = 0$. The second condition suggests that modified Bessel function should indicate the required variation in the cladding in addition to ruling out $I_m(|k|r)$ by choosing $B_2 = 0$. In other words, $k = (n_2^2 k_0^2 - \beta^2)^{\frac{1}{2}} = k_2$ is required to be imaginary in the region $(r \ge a)$ and the

modified Bessel function $K_m(|k|r)$ (Hankel) must be chosen in this region where the refractive index n_2 is slightly higher. Choosing A=α=0 in Eq. (2.23), we find the final solution for E_z as:

$$E_z = \begin{cases} A_1 J_m(k_1 r) Sin(m\varphi) \exp(i(\omega t - \beta z)) & r \le a \\ B_1 K_m(|k_2|r) Sin(m\varphi) \exp(i(\omega t - \beta z)) & r \ge a \end{cases} \quad (2.25)$$

The same procedure can be followed to solve the wave equation for H_z propagating along the fiber axis in the z direction.

$$H_z = \begin{cases} C_1 J_m(k_1 r) Cos(m\varphi) \exp(i(\omega t - \beta z)) & r \le a \\ D_1 K_m(|k_2|r) Cos(m\varphi) \exp(i(\omega t - \beta z)) & r \ge a \end{cases} \quad (2.26)$$

Choosing the cosine dependence for H_z instead of sine enables continuity of all tangential field components at $r = a$ between the core and the cladding. Using Eqs. (2.3) and (2.4), the transverse field components can be found in terms of the first derivatives of the z-components of E and H:

$$E_r = \frac{-i}{k^2}\left(\beta \frac{\partial E_z}{\partial r} + \omega\mu \frac{1}{r}\frac{\partial H_z}{\partial \varphi}\right) \quad (2.27)$$

$$E_\varphi = \frac{-i}{k^2}\left(\beta \frac{1}{r}\frac{\partial E_z}{\partial \varphi} - \omega\mu \frac{\partial H_z}{\partial r}\right) \quad (2.28)$$

$$H_r = \frac{-i}{k^2}\left(\beta \frac{\partial H_z}{\partial r} - \omega\varepsilon \frac{1}{r}\frac{\partial E_z}{\partial \varphi}\right) \quad (2.29)$$

$$H_\varphi = \frac{-i}{k^2}\left(\beta \frac{1}{r}\frac{\partial H_z}{\partial \varphi} + \omega\varepsilon \frac{\partial E_z}{\partial r}\right) \quad (2.30)$$

The boundary condition on the tangential components of **E** and **H** requires that E_z, H_z, E_φ, and H_φ be equal at $r = a$ for the components of the fields inside and

outside of the core. The equality of these field components at r = a leads to an eigenvalue equation whose solutions determine the propagation constant β for the fiber modes. The eigenvalue equation can be written as [2]:

$$\left[\frac{J_m^{'}(u)}{uJ_m(u)}+\frac{K_m^{'}(w)}{wK_m(w)}\right]\left[\frac{J_m^{'}(u)}{uJ_m(u)}+\frac{n_2^2}{n_1^2}\frac{K_m^{'}(w)}{wK_m(w)}\right]=m^2\left(\frac{1}{u^2}+\frac{1}{w^2}\right)\left(\frac{1}{u^2}+\frac{n_2^2}{n_1^2}\frac{1}{w^2}\right) \tag{2.31}$$

where u and w are normalized transverse propagation constants defined as:

$$u=ak_{_1}=a(n_1^2k_0^2-\beta^2)^{\frac{1}{2}},\ w=a|k_2|=a(\beta^2-n_2^2k_0^2)^{\frac{1}{2}} \tag{2.32}$$

The prim functions, $J_m^{'}$ and $K_m^{'}$, denote that their derivatives are taken with respect to the arguments. In practical optical fibers, Eq. (2.31) can be greatly simplified by the weakly guiding approximation which is $n_1 \approx n_2$. Therefore, the eigenvalue equation for optical fibers will be:

$$\frac{J_m^{'}(u)}{uJ_m(u)}+\frac{K_m^{'}(w)}{wK_m(w)}=\pm m\left(\frac{1}{u^2}+\frac{1}{w^2}\right) \tag{2.33}$$

In general, Eq. (2.33) provides several solutions for each integer value of m. Each eigenvalue corresponds to one mode which the fiber can support. For m = 0, these modes are analogous to the transverse-electric (TE) and transverse-magnetic (TM) modes of a planar waveguide since the axial component of the electric field E_z and the magnetic field H_z vanishes, i.e. $A_1=B_1=0$ in Eq. (2.25) and $C_1=D_1=0$ in Eq. (2.26) respectively. In TE modes, in addition to H_z, the only nonzero field components will be E_φ and H_r; however, the only nonzero field components in TM modes are E_r, H_φ and E_z. For $m \neq 0$, the fiber modes are hybrid, that is, E_z, H_z and all the other components of the electromagnetic field are nonzero. Physically speaking, this case corresponds to an oblique ray which cannot maintain purely transverse electric and magnetic field components. These modes are designated as

either EH or HE modes depending on the characteristics of the eigenvalue equation. Eq. (2.33) with positive right-hand side is the eigenvalue equation for EH modes; however, this is the equation for HE modes with negative right hand side. By defining a new integer variable, Eq. (2.33) can be modified to express all modes eigenvalue equation as [2]

$$u\frac{J_{l-1}(u)}{J_l(u)} = -w\frac{K_{l-1}(w)}{K_l(w)} \qquad l = \begin{cases} 1 & TE,TM \\ m+1 & EH \\ m-1 & HE \end{cases} \tag{2.34}$$

In addition, a set of degenerate EH, HE, TE, and TM modes can combine to form a new composite mode with the same eigenvalue Eq. (2.34). The composite mode is referred to as the LP mode because its electric field is linearly polarized in the transverse plane. Although the LP modes can be obtained by simple additions of the mode functions, they can also be deduced directly from the wave Eq. (2.18) [3]. In practice, the LP modes are readily identified by their transverse intensity profile. The LP system is a simplified method to describe modes in weakly guiding fibers. A graphical method is usually demonstrated for solving the eigenvalue Eq. (2.34) [4]. An important parameter for each mode in a fiber is the normalized frequency often called the V number determined by

$$\mathrm{V} = (u^2 + w^2)^{\frac{1}{2}} = ak_0(n_1^2 - n_2^2)^{\frac{1}{2}} \tag{2.35}$$

The V number is used with Eq. (2.34) to determine cutoff conditions for the modes, propagation constants, and information on power confinement in a fiber. The value of u when $w = 0$ determines the cutoff frequency $\mathrm{V_c}$ for a given mode.

2.2.1 Cutoff Conditions in Single-Mode Fiber

For a given mode, cutoff can be determined from Eq. (2.34) by using $w = 0$ meaning $u = \mathrm{V}$ by Eq. (2.35). Therefore, the cutoff condition is obtained

$$\frac{\mathrm{V}\, J_{l-1}(V)}{J_l(\mathrm{V})} = 0 \tag{2.36}$$

which is the cutoff condition for a given mode. Using the small argument approximation, i.e. $J_l(\mathrm{V}) \approx \frac{1}{l!}(\frac{\mathrm{V}}{2})^2$, the special case of V=0 results $l = 0$ which corresponds to the mode LP_{01} (in LP_{lm} mode system) or HE_{11} (m=n=1, where n is the mode rank or radial mode number which is greater than or equal to one) according to Eq. (2.34). Other zeros of the cutoff condition Eq. (2.36) occur when $J_{l-1}(\mathrm{V}) = 0$. Each Bessel function zero is considered; thus, the mode with the cutoff occurring at that value of V will be established. The first zero is 2.405 for J_0, i.e. $J_0(2.405) = 0$, which indicates that $l = 1$ in Eq. (2.34). In other words, LP_{11} in LP mode designation or the degenerate modes TE_{01}, TM_{01} and HE_{21} have cutoff at V=2.405 which is the first instance (n=1) in which any of these modes occur as V increases with the given value of m. Since values of V for a given mode occurs over the range $\mathrm{V_c} \le \mathrm{V} \le \infty$, where $\mathrm{V_c}$ is the value of V at the cutoff for that mode, the single-mode fiber is designed such that all higher-order modes are cut off at the operating wavelength of the HE_{11} mode or LP_{01} known as the fundamental mode of the fiber. A fiber with a large value of V supports many modes, in other words, as V is reduced, the number of modes decreases rapidly. A rough estimate of the number of modes for a multimode fiber is given by $\frac{\mathrm{V}^2}{2}$ [5]. Below the certain value of V=2.405, all modes except the HE_{11} (LP_{01}) mode reach cutoff; therefore, such single-mode fibers support a single mode HE_{11}.

In situations involving single-mode fibers, where the operating wavelength is fixed, it is often more convenient to specify the cutoff wavelength λ_c since wavelength is a directly measurable quantity. The cutoff wavelength for any mode is defined as the maximum wavelength at which that mode propagates. From Eq. (2.35), the two parameters λ_c and V_c for each LP mode are related through

$$\lambda_c = \frac{2\pi a}{V_c}(n_1^2 - n_2^2)^{\frac{1}{2}} = \frac{\lambda V}{V_c} \tag{2.37}$$

Therefore, the operating wavelength for a single-mode fiber (supporting LP_{01}) must be greater than the cutoff wavelength for the next mode LP_{11}. The result is a fiber that rejects all the higher order modes and conducts only the fundamental mode HE_{11} (LP_{01}) which travels exactly along the core of the fiber with the wavelength

$$\lambda > \frac{2\pi a}{V_c}(n_1^2 - n_2^2)^{\frac{1}{2}} \tag{2.38}$$

For a typical value $n_1 - n_2 = 0.005$ for the index difference, and $a = 4\mu m$, Eq. (2.37) indicates that $\lambda_c = 1.2\mu m$ so the fiber supports a single mode only for the wavelength $\lambda > 1.2\mu m$. If we want to work with light at a shorter wavelength in a fiber, we can either decrease the core radius a or make n_1 as close to n_2 as possible. In practice, a fiber with core radius below 2μm supports a single mode in the visible region.

The field distribution corresponding to the fundamental mode HE_{11} has three nonzero components E_x, E_y, and E_z or in cylindrical coordinates E_r, E_φ, E_z obtained using Eqs. (2.25)-(2.30). In a single-mode fiber, the axial components E_z and H_z are very small especially in the condition $n_1 \approx n_2$; hence, among all the electromagnetic field components, either E_x or E_y dominates. Therefore, the

fundamental fiber mode HE_{11} is approximately linearly polarized in either the x or y direction for weakly guiding fiber for which both E_z and H_z are nearly zero. In this respect, a single-mode fiber is not completely single mode since it can simultaneously support two modes of orthogonal polarizations corresponding to the fundamental mode HE_{11} (LP_{01}) [6]. For a linearly polarized mode, one of the transverse components can be considered as zero. By setting E_y=0, the E_x component of the electric field for the fundamental mode is obtained by [7]

$$\mathrm{E}_x = \mathrm{E}_0 \exp(-i\beta z)\begin{cases} J_0(\frac{ur}{a}) & r \le a \\ \frac{J_0(u)}{K_0(w)} K_0(\frac{wr}{a}) & r \ge a \end{cases} \tag{2.39}$$

where E_0 is a constant related to the power carried by the mode and the coordinate transformation $\mathrm{E}_x = \mathrm{E}_r \cos\varphi - \mathrm{E}_\varphi \sin\varphi$ is used. It is evident that the dominant component of the corresponding magnetic field is given by $\mathrm{H}_y = n_2\sqrt{\varepsilon_0/\mu_0}\,\mathrm{E}_x$. From Eq. (2.39), it is known that the fundamental mode LP_{01} intensity varies with radius as $J_0^2(\frac{ur}{a})$ inside the core, and as $K_0^2(\frac{wr}{a})$ in the cladding. These two functions connect at $r = a$ to form the composite intensity profile. The resultant field distribution is cumbersome to use in practice and it is often approximated by a Gaussian function given by

$$\mathrm{E}_x = \mathrm{E}_{0g} \exp(\frac{-r^2}{r_0^2}) \exp(-i\beta z) \tag{2.40}$$

where the width r_0 is known as the mode field radius or also referred to the spot size. This Gaussian distribution is determined by fitting the exact distribution in Eq. (2.39) or by following a variational procedure [8]. The quality of fit is

generally quite good for values of V in the neighborhood of V=2. The radius r_0 is defined as the radial distance from the core center of the fiber to $1/e^2$ point of the Gaussian intensity profile. It is evident that this is the same distance measured to $1/e$ point of the Gaussian electric field profile. Although r_0 can be determined directly from the plotting of the Gaussian function, it can also be approximated analytically to better than 1% accuracy for 1.2<V<2.4 as [9].

$$\frac{r_0}{a} = 0.65 + 1.619\mathrm{V}^{\frac{-3}{2}} + 2.879\mathrm{V}^{-6} \tag{2.41}$$

A simpler formula was also obtained by using a variational method [10]

$$\frac{r_0}{a} \approx \frac{1}{\sqrt{\mathrm{LnV}}} \tag{2.42}$$

As seen, r_0 decreases with increasing V, thus reflecting the principle of tighter mode confinement with frequency. The mode field radius is an important aspect of a single-mode fiber and it is specified at a given wavelength instead of the core size of the fiber. The effective core area, defined as $\mathrm{A}_{\mathrm{eff}} = \pi r_0^2$, is an important specification for optical fibers as it determines how tightly light is confined to the core. With smaller values of $\mathrm{A}_{\mathrm{eff}}$, the nonlinear effects are stronger which will be discussed later.

Apart from the fact that the intensity pattern is easier to visualize with the Gaussian mode approximation, it is also easier to use the Gaussian function in constructing models of fiber performance such as mode confinement provided by the mode field radius. Mode confinement states requirements and tolerances for coupling between the fiber and a light source or even between two fibers. The confinement factor Γ gives the fraction of the power contained in the core of the fiber and is defined as

$$\Gamma = \frac{P_{core}}{P_{total}} = \frac{\int_0^a |E_x|^2 rdr}{\int_0^\infty |E_x|^2 rdr} = 1 - \exp(\frac{-2a^2}{r_0^2}) \quad (2.43)$$

Eqs. (2.41)-(2.43) determines the fraction of the mode power contained inside the core for a given value of V. Nearly 75% of the mode power is confined in the core for V=2 whereas it drops to 20% for V=1. Therefore, most telecommunication single-mode fibers are designed to work in the condition that 2<V<2.4.

2.2.2 Types of Single-Mode Optical Fibers

Single-mode optical fibers are preferred for long haul, large bandwidth and for use with integrated optic components. As said before, single-mode fiber is not completely single mode since it can simultaneously support two modes of orthogonal polarizations corresponding to the fundamental mode HE_{11} (LP_{01}) [6]. In addition, these two orthogonally polarized modes are degenerate under ideal conditions because they have the same propagation constant. In practice, however, this degeneracy breaks slightly due to some irregularities such as random variations in the core shape and its size along the length of the fiber. This mixes randomly the two polarization components, and scrambles the polarization of the incident light as it propagates through the single-mode fiber. Nevertheless, for some applications, it is required that fibers maintain state of polarization for transmission light. Such fibers called polarization-maintaining fibers or polarization-preserving fibers can meet this requirement [11]. Random fluctuations in the core shape and size of the fiber are not the governing parameters in state of polarization in these fibers since such fibers can preserve the linear polarization if the light is launched with its polarization along one of the principal axes of the fiber. Assuming that the incident light is polarized along a

principal axes coincided with the x axis, the electric field for the fundamental mode HE_{11} propagating in the fiber is approximately given by

$$\mathbf{E} = \mathbf{X}\ E_0\ F(x, y)\ \ \exp(-i\beta(\omega)z) \tag{2.44}$$

where as before the fundamental fiber mode is often approximated by a Gaussian distribution of the form

$$F(x, y) \approx \exp(\frac{-r^2}{r_0^2}) \tag{2.45}$$

Where $r^2 = x^2 + y^2$. The propagation constant $\beta(\omega)$ is yield by solving the eigenvalue Eq.(2.34). Frequency dependence of $\beta(\omega)$ results not only from the frequency dependence of n_1 and n_2, referred to as the material dispersion but from the frequency dependence of k_1 known as waveguide dispersion. Generally, the waveguide dispersion is relatively smaller except near the zero-dispersion wavelength λ_D where the two dispersion phenomena become comparable. Dispersion does not vanish at $\lambda=\lambda_D$ however dispersion of the group velocity which is responsible for pulse broadening vanishes [12].

Dispersion is a detrimental effect in single-mode fibers even when the nonlinear effects are not important. It is a phenomenon called chromatic dispersion in which the propagating velocity of an electromagnetic wave depends on the wavelength. Since different frequency components of a signal travel at different speed due to chromatic dispersion, the signal will be degraded by wavelength – dependent pulse spreading. To solve this problem, single-mode fiber has gone through a continuing evolution for several decades. Using the dependence of the waveguide dispersion on fiber-design parameter, we can shift the zero-dispersion wavelength in the vicinity of 1550 nm where the fiber loss is minimum, as cited in section 1.3.2. Such fibers with the zero-dispersion wavelength λ_d at 1550 nm is

known as dispersion-shifted fibers and have found applications in optical communication systems [13]. Therefore, depending on whether the dispersion is zero or not at 1550 nm, fibers are commercially known by names as zero and nonzero dispersion shifted fibers, respectively. Although dispersion does not vanish at the wavelength λ_d, dispersion of group velocity is zero at this wavelength. The group velocity is the envelope velocity at which an optical signal pulse moves. Erbium doped optical fiber amplifiers which offer high gain around 1550 nm make nonzero dispersion shifted fibers undesirable due to its very high dispersion at the commercial wavelength of 1550 nm. In addition, although dispersion shifted fiber operation is most desirable from the viewpoint of signal pulse broadening at the wavelength 1550 nm, this fiber exhibits some other performance which preclude its applications. For example, at most one channel can be located at the zero dispersion wavelength. Besides, in dense wavelength division multiplexed system where there are multiple closely spaced wavelengths, some serious nonlinearities such as self-phase modulation, cross-phase modulation and four-wave mixing can cause pulse broadening. The technique of dispersion management provides a solution to this drawback. In fact, it combines fibers with various characteristics in a manner that the average dispersion of group velocity in the entire fiber is very low whereas this dispersion for each fiber section is large enough to cause four-wave mixing effects to be negligible [14]. In such a fiber, called a dispersion compensating fiber, dispersion is completely compensated when the dispersion of group velocity is set to zero. The development of dispersion compensating fibers accelerated after the advent of optical amplifiers [15], [16]. On the other hand, a single-mode dispersion compensating fiber suffers from some problems. Firstly, it has high loss ($\alpha \approx 0.5$ dB/km) in the wavelength

region 1550 nm. Secondly, 1 km of this fiber compensates dispersion for about 10 km of standard fiber. Finally, due to a relatively small mode diameter, the optical intensity is high at a given input pump power, which results in enhanced nonlinear effects. Two-mode dispersion compensating fibers having high-order mode with normalized cutoff frequency near 2.5 ($V \approx 2.5$) have been used for solving, to some extent the problems of the single-mode dispersion compensating fiber [17], [18].

2.3 Fiber Losses

Fiber losses, in addition to dispersion, indicate another important factor that inherently limits the performance of optical communication systems since they reduce signal power during transmission inside an optical fiber. Before the advent of optical amplifiers, optical communications was practical only after reducing loss to an acceptable level [19]. Even now, low-loss fibers are usually chosen in optical communications since fiber losses still play a part in determining the spacing between amplifiers. Although there are several loss factors corresponding to each element in addition to loss of splicing connectors in an optical system, only losses associated with optical fibers will be discussed here. The fiber loss mechanisms are categorized as either intrinsic or extrinsic depending on whether they are associated with the fundamental material properties of the glass used in the fiber manufacturing process, or not, respectively. In other words, intrinsic losses correspond to losses that arise from fused silica used to make fibers whereas extrinsic losses are related to impurities within the silica. The optical loss in glass fibers can also be classified as absorption, scattering, and geometric effects. In a pure silica glass, there are three dominant sources of

important intrinsic loss at visible and near-infrared wavelength. According to the electronic and vibrational resonances associated with certain molecules, any material absorbs a specific wavelength. These resonances include electronic resonances in the ultraviolet (UV) region $(\lambda < 400nm)$ and vibrational resonances in the infrared (IR) region $(\lambda > 700nm)$ and the mechanism of Rayleigh scattering. These three mechanisms of intrinsic loss are wavelength dependent. For signal transmission, the suitable wavelength can be determined by the combination of these effects.

The electronic resonance centered at $\lambda = 0.1\mu m$ causes absorption effects to become appreciable in the visible wavelength region but negligible in the near-infrared [20]. It tends to shift toward the infrared region when dopant material is added [21]. Lattice vibrational mode resonances are centered between 700 and 1100 nm (IR) wavelength region. Infrared absorption extends into the near-infrared region as a result of anharmonic coupling which occurs between the numerous vibrational modes. As a consequence, dopants with lighter atomic masses results in shorter resonant wavelength; therefore, light dopants such as B_2O_3 have not been used in fibers with operational wavelength between 1200 and 1800 nm. On the other hand, dopants such as P_2O_5 may bond with OH ions to produce a stretch resonance by approximately 1650 nm which results in substantial absorption at this wavelength. Thus, in regions where the mode power is high, it is usually desirable not to use P_2O_5 unless the OH ion concentration can be reduced to very low levels. The power loss associated with IR absorption can be obtained by

$$\alpha_{IR} = \mathrm{A}\exp(-\frac{\mathrm{a}_{\mathrm{IR}}}{\lambda}) \tag{2.46}$$

in which λ is the wavelength in μm, A and a_{IR} are constants which for Sio_2 glass fiber are $A = 7.01\times10^{11}$ (dB/km) and $a_{IR} = 48.48\mu m$ [21]. Special precautions are taken during the fiber-fabrication process to ensure an OH-ion level of less than one part in one hundred million since OH ion as the most important impurity affecting fiber loss has a fundamental absorption peak at approximately 2730 nm [22]. OH-ion combination tones and its harmonic with silica causes the three spectral peaks at wavelengths 1390, 1240, and 950 nm in the loss spectrum of a single-mode fiber [23]. Even an OH concentration of 1 part per million can cause a loss of about 50 dB/km at 1390 nm. In modern fibers, the OH ion concentration is reduced to below 10^{-8} to lower the peak of the wavelength 1390 nm below 1 dB. OH-ions are present due to the residual water vapor in silica. In a new kind of fiber, called the dry fiber or also known as the All-Wave fiber in trade, the 1390 nm peak almost disappears by reducing the OH-ion concentration [24]. This fiber can be used in wavelength division multiplex signal transmission system over the entire 1300-to 1650 nm wavelength region.

There are some models of Rayleigh scattering process in glass. In a microscopic description, pure silica has an amorphous nature; therefore, it is possible that some irregularities happen in its basic structure [25]. The heat applied during silica fiber manufacturing provides energy for Sio_2 molecules to move randomly through the entire molten glass. During the glass fiber manufacturing process, the glass is rapidly cooled leading to random molecular locations for Sio_2 molecules in the frozen silica fiber. Therefore, the material density indicates random microscopic variations leading to variations of refractive index. These local random variations in density also act as scattering centers. Such scatters are of dimensions much less than the incident wavelength. Objects like

this satisfy the condition called Rayleigh criterion. Rayleigh scattering processes are classically described by incident light exciting atomic dipoles into oscillation which results in some absorption of the incident power. Then, each oscillating dipole reradiates so that the far-fields emitted from an excited atomic dipole oscillator of length dl<<λ along the z axis can be expressed as [26]

$$\mathrm{E}_{\theta} = \eta_0 \mathrm{H}_{\varphi} = \frac{-\mathrm{p}\sin\theta}{\varepsilon_0^2 \lambda^2 \mathrm{R}} \exp\left(\frac{-2\pi\ \mathrm{iR}}{\lambda}\right) \tag{2.47}$$

where $\eta_0 = \sqrt{\mu_0 / \varepsilon_0} = 377\Omega$, is called the intrinsic impedance of medium (supposed vacuum) where light propagates. θ is the angle between propagation vector of the scattered light with the dipole direction which is the same as the electric field direction of the incident light. Thus, as a result of the reradiating effect, more of the incident light power is scattered when the frequency of the light increases. According to Poynting's theorem Eq. (2.15) and the aforementioned equation, the radiated power density at a given value of θ can be deduced to be proportional to the fourth power of the frequency. Experimentally, Rayleigh scattering is determined in decibels per kilometer through

$$\alpha_R = \frac{\mathrm{B}}{\lambda^4} \tag{2.48}$$

where B is the Rayleigh scattering coefficient in the range of 0.7-0.9 dB/(km.μm^4) corresponding to the loss $\alpha_R = 0.12 - 0.16$ dB/km at the wavelength 1550 nm. Depending on the constituents of the core of fiber, it is intrinsic ultimate limit on optical fiber loss dominant near 1550 nm. At near-infrared wavelengths, the UV resonance due to electronic resonance origin is negligible so that the net intrinsic loss of material absorption and Rayleigh scattering will be as:

$$\alpha_{\mathrm{int.}} = \mathrm{A}\exp\left(-\frac{\mathrm{a_{IR}}}{\lambda}\right) + \frac{\mathrm{B}}{\lambda^4} \tag{2.49}$$

Using the values of A and B, it can be shown that the minimum loss occurs at approximately $\lambda_{min} \approx 0.03 a_{IR}$ μm [27]; hence, Rayleigh scattering expressed by the second term in the above equation is the dominant intrinsic loss mechanism in the low-loss wavelength region about 1550 nm depicted before in the figure (1.1). On the other hand, some glass which may be suitable for making ultralow-loss fibers, Rayleigh scattering loss α_R can be as low as 0.05 dB/km at 1550 nm [28]. Rayleigh scattering can also be reduced to 0.01 dB/km at the wavelength of 3000 nm; however, silica fibers are not suitable in this wavelength region due to infrared absorption which is an effective loss beyond 1600 nm [29].

Because of the other loss sources such as splicing and cabling losses, total loss of fibers used in optical systems are slightly larger. Other loss sources such as bending of fiber and scattering of light at the core-cladding interface may also contribute to the total loss of optical fibers [30].

2.4 Nonlinear Effects in Optical Fibers

When high intensity light passes through optical fibers or bulk materials, various nonlinear effects may be observed [31]. The nonlinear effects commonly observed are second harmonic generation (SHG), third harmonic generation (THG), four wave mixing (FWM), stimulated Raman scattering (SRS), stimulated Brillouin scattering (SBS), and many others. Nonlinear effects are related to the anharmonic motion of the bound electrons under the influence of an applied electromagnetic field. With an intense electromagnetic field, nonlinear response of the refractive index in an optical fiber is more obvious. In practice, the largest electric fields obtained in matter fall into the range of 10^6 V/cm in which most forms of matter exhibit electrical breakdown. In addition, an electron bound to an

atom or molecule or moving through a solid or dense liquid, experiences electric fields in the range of 10^9 V/cm because over distances which are the order of an angstrom around the electron, the change in electrostatic potential can be several electron volts. Therefore, the external laboratory fields are very small compared to the electric fields naturally experienced by the electrons in the atom and molecule structures from which dense matter is constructed. In this condition, one can expand the dipole electric moment per unit volume, P(r,t), in a Taylor series in powers of the macroscopic field E(r,t) at the same point and at the same time.

$$P_\alpha(r,t) = P_\alpha(E=0,r,t) + \sum_\beta \left(\frac{\partial P_\alpha}{\partial E_\beta}\right) E_\beta + \frac{1}{2!}\sum_\beta \sum_\gamma \left(\frac{\partial^2 P_\alpha}{\partial E_\beta \partial E_\gamma}\right) E_\beta E_\gamma + \frac{1}{3!}\sum_\beta \sum_\gamma \sum_\delta \left(\frac{\partial^3 P_\alpha}{\partial E_\beta \partial E_\gamma \partial E_\delta}\right) E_\beta E_\gamma E_\delta + \ldots \quad (2.50)$$

where α, β, γ, δ range over the Cartesian components x, y, and z. Then the αth Cartesian component of the dipole moment per unit volume, $P_\alpha(r,t)$ is a function of the three Cartesian components of the external electric field. In our situation, the first term, $P_\alpha(E=0,r,t)$, which is the electric dipole moment per unit volume in zero external electric field, vanishes. In other words, any electric dipole moments are due to the external electric field. It is common to show this result as

$$\mathbf{P} = \varepsilon_0 [\, \chi^{(1)} \mathbf{.}\, \mathbf{E} + \chi^{(2)} \mathbf{:}\, \mathbf{EE} + \chi^{(3)} \vdots\, \mathbf{EEE} + \ldots \,] \quad (2.51)$$

where ε_0 is the vacuum permittivity and $\chi^{(i)}$ (i=1,2,….) is the $(i+1)^{th}$ order tensor susceptibility. The operations denoted by .,:,⋮ are convolutions which show summation over repeated indexes. The linear susceptibility $\chi^{(1)}$ represents the dominant contribution which relates linearly **E** to **P** , while the second order

susceptibility $\chi^{(2)}$ is the lowest nonlinear susceptibility responsible for second-order nonlinear effects such as second harmonic generation and sum-frequency generation. Since both **P** and **E** are vectors and so odd under inversion symmetry, the value of $\chi^{(2)}$ must be zero in any centrosymmetric and isotropic material which is left invariant in form under inversion. Therefore, $\chi^{(2)}$ diminishes in silica glasses where there are symmetrical molecules of SiO_2. That is the second-order nonlinear effects can not be exhibited in optical silica fibers. Then the lowest order nonlinear effects originate from the 3rd order susceptibility $\chi^{(3)}$, which is responsible for phenomena such as third harmonic generation, four-wave mixing and nonlinear refraction. These phenomena mentioned in the 3rd order susceptibility $\chi^{(3)}$ are elastics as there is no energy exchanged between the electromagnetic fields and matter. They are due to the dependence of the refractive index on the input light power. However, there are also third-order effects occurring because of the inelastic scattering effect.

This class of nonlinear effects results from stimulated Brillouin scattering (SBS) and stimulated Raman scattering (SRS) in which the optical field transfer part of its energy to the nonlinear medium. They can be explained quantum-mechanically as scattering of a pump photon to a lower energy photon called a Stokes photon by generating a phonon with energy equal to the energy reduction of the initial photon. The main difference between the two is the type of interval mode involved. SRS involves nonpropagating collective modes as optical phonons in the medium whereas SBS involves low-frequency propagating acoustic wave phonons in it. Another fundamental difference is that SBS occurs only in the backward direction which is the opposite direction respect to the incident light. However, SRS is able to occur in both forward and backward directions although

SRS dominates in the forward direction where SRS is in the same direction as the incident light. The other difference is that the downshifted scattered light is about 10 GHz for SBS but 13 THz for SRS with respect to the incident light frequency in the SMF. Finally, the Brillouin-gain spectrum bandwidth is less than 100 MHz which is very narrow when comparing with the Raman-gain spectrum bandwidth which is more than 20 to 30 THz. SBS has been shown to provide harmful effects in optical fiber telecommunication system due to its low threshold power, however it has also been indicated SBS is useful for applications in Brillouin amplifiers, Brillouin/erbium fiber lasers (BEFL), and Brillouin fiber lasers (BFL) which is of particular interest in this thesis. Principles of SBS generation will be considered later; it describes the implication of Brillouin Stokes in the BFL generation.

2.5 Principles of Stimulated Brillouin Scattering (SBS)

As mentioned in the last section, the physical process of SBS can be explained by a nonlinear interaction between pump wave which is the incident light, Stokes wave or scattered light, and an acoustic wave generated through a process known as electrostriction. Once the Brillouin scattered wave at the frequency ω_s is spontaneously generated, it beats with the pump wave at the frequency ω_p and produces a beat frequency $(\omega_p - \omega_s)$ which is exactly equal to the acoustic wave frequency ω_a. Consequently, this beat acts a source to amplify the amplitude of the acoustic wave, which in turn amplifies the amplitude of the Brillouin scattered wave as a positive feedback. SBS can ultimately transfer all pump power to the Brillouin scattered wave power which is detrimental in optical transmission communication systems. The electrostriction phenomenon causes all electrical non-conductors or dielectrics to change their shape under the application

of an electric field. Brillouin scattering may be understood via scattering of a pump photon by a phonon which is a unit of energy and momentum for the acoustic or sound wave. The conservation of energy and linear momentum during Brillouin scattering demands following equations for the frequencies and wave vectors

$$\omega_p = \omega_s + \omega_a \tag{2.52}$$

$$\mathbf{k}_p = \mathbf{k}_s + \mathbf{k}_a \tag{2.53}$$

where the indexes p, s, and a refer to pump, scattered, and sound waves, respectively. The sound frequency is very small compared to the light frequency, that is $\omega_a << \omega_p, \omega_s$; therefore, $\omega_p \approx \omega_s$, $k_p = k_s$ and it can be deduced that

$$k_a^2 = 4k_p^2 \sin^2\frac{\gamma}{2} \tag{2.54}$$

where γ indicates the angle between the pump and scattered wave vectors, k_p and k_s, respectively . Regarding $k_a = \frac{\omega_a}{v_a}$, and $k_p = \frac{\omega_p}{v_p}$, it can be obtained

$$\omega_s = \omega_p(1 - 2\frac{v_a}{v_p}\sin\frac{\gamma}{2}) \tag{2.55}$$

which can also be described classically via scattering of the pump light by a moving grating with the sound velocity v_a in Doppler effect. v_p is the pump light wave velocity in the medium. It is clear that the Brillouin frequency shift, which is equal to ω_a, is zero when the pump and scattered fields propagate in the same direction and has its maximum value $2\frac{v_a}{v_p}\omega_p$ when the scattered light, the Brillouin Stokes, propagates in the opposite direction $(\gamma = \pi)$ which is our case happening in optical fibers.

The propagation of elastic waves in a dissipative medium can be described by a material density function ρ [kg/m^3] satisfying the wave equation driven through electrostriction phenomenon as

$$v_a^2 \nabla^2 \rho - \frac{\partial^2 \rho}{\partial t^2} + \Gamma \nabla^2 \frac{\partial \rho}{\partial t} = \nabla \bullet \mathbf{f} \tag{2.56}$$

where $f = \frac{1}{2} \gamma_e \nabla E^2$, the force per unit volume of the medium, produces the density fluctuation due to light propagation in the medium [32], [33]. $v_a = \sqrt{Y/\rho}$ is the speed of the acoustic wave or longitudinal sound velocity in the medium and $\Gamma = \eta_{11} / \rho_0$ [m^2/s] is known as sound damping factor in the region. Y [Pa] is Young's modulus, η_{11} [Pa s] is the bulk viscosity coefficient of the optical fiber, and ρ_0 is the unperturbed density. The parameter γ_e called the electrostriction coefficient is the strength of the electrostriction effect. The nonlinear polarization for SBS can be obtained by using Eq. (2.6) for the electric displacement vector **D** and Taylor's expansion of the permittivity coefficient as:

$$\mathbf{D} = \varepsilon \ \mathbf{E} = \varepsilon_0 \mathbf{E} + (\rho - \rho_0) \left[\frac{\partial \varepsilon}{\partial \rho} \right]_{\rho = \rho_0} \mathbf{E} \tag{2.57}$$

In comparison to the relation $\mathbf{D} = \varepsilon_0 \mathbf{E} + \mathbf{P_L} + \mathbf{P_{NL}}$ which can be deduced by Eqs. (2.6) and (2.51), the nonlinear polarization for Brillouin scattering is in the form

$$\mathbf{P}_{\mathrm{NL}} = \frac{\gamma_e}{\rho_0} \rho \mathbf{E} \tag{2.58}$$

where the definition $\gamma_e = \rho_0 [\partial \varepsilon / \partial z]_{\rho = \rho_0}$ has been used.

Thus, the electric field can be evaluated by Eq. (2.8) and the above nonlinear polarization for SBS as the following

$$\nabla^2 E - \frac{1}{v^2} \frac{\partial^2 E}{\partial t^2} = \frac{\mu_0 \gamma_e}{\rho_0} \frac{\partial^2 \rho E}{\partial t^2} \tag{2.59}$$

In order to solve the coupled Eqs. (2.56) and (2.59), it is common to suppose that the pump, Stokes, and acoustic waves are plane waves propagating in the z direction assumed to be the axis of the fiber [34]. Hence, the supposed linearly co-polarized pump and Stokes fields and the sound wave with the propagation vectors $\mathbf{k}_p=k_p\,\mathbf{z}$, $\mathbf{k}_s=k_s\,(-\mathbf{z})$, and $\mathbf{k}_a=k_a\,\mathbf{z}$ respectively, have the forms

$$E_p(z,t)=\frac{1}{2}E_{0p}(z)e^{i(\omega_p t-k_p z)}+c.c. \tag{2.60}$$

$$E_s(z,t)=\frac{1}{2}E_{0s}(z)e^{i(\omega_s t+k_s z)}+c.c. \tag{2.61}$$

$$\rho(z,t)=\rho_0+\frac{1}{2}Ae^{i(\omega_a t-k_a z)}+c.c. \tag{2.62}$$

in which c.c. denotes the complex conjugate of the first term with the assumption that the amplitudes E_{0p}, E_{0s}, and A are not functions of time regarding the steady-state regime. Assuming that the electric field E is obtained by superposition of the electric fields E_p and E_s, the right hand of Eq. (2.56) will be

$$\nabla\bullet\mathbf{f}=\frac{\gamma_e}{4}\nabla^2E^2=\frac{-\gamma_e(k_p+k_s)^2}{4}[E_{0p}E_{0s}^{*}e^{i[(\omega_p-\omega_s)t-(k_p+k_s)z]}+c.c.] \tag{2.63}$$

where the rapidly oscillating terms contributing at frequencies $2\omega_1$, $2\omega_2$, and $\omega_1+\omega_2$ are neglected by regarding time averaging. Using Eqs. (2.56), (2.62), and (2.63) yields:

$$A=\frac{(k_p+k_s)^2\gamma_e E_{0p}E_{0s}/2}{v_a^2k_a^2-i\Gamma k_a^2(\omega_p-\omega_s)-(\omega_p-\omega_s)^2} \tag{2.64}$$

Now, in order to find the electric fields, it is common to use an assumption called the Slowly Varying Envelope Approximation (SVEA), that is the electric fields E_p

and E_s exhibit slow variations over the medium length such that their second derivatives with respect to z are negligible, in other words,

$$\left| k \frac{\partial \mathrm{E}_{0\mathrm{p,s}}}{\partial \mathrm{z}} \right| >> \left| \frac{\partial^2 \mathrm{E}_{0\mathrm{p,s}}}{\partial z^2} \right| \tag{2.65}$$

in which $E_{0p,s}$ shows the amplitude E_{0p} or E_{0s}. For a plane wave $k = \frac{2\pi}{\lambda}$, so that the SVEA condition will be as:

$$\left| \frac{\partial \mathrm{E}_{0\mathrm{p,s}}}{\partial \mathrm{z}} \right| >> \left| \lambda \frac{\partial}{\partial \mathrm{z}} \left(\frac{\partial \mathrm{E}_{0\mathrm{p,s}}}{\partial \mathrm{z}} \right) \right| \tag{2.66}$$

Physically speaking, over a distance of one wavelength, the magnitude of the slope of the electric field is much more than the change in the slope of the field. Thus, in this approximation, the first term of Eq. (2.59) can be approximated as

$$\nabla^2 \mathrm{E}_{\mathrm{p,s}} = \frac{\partial^2 \mathrm{E}_{\mathrm{p,s}}}{\partial z^2} \approx \frac{1}{2} \left(\mp i 2 k_{\mathrm{p,s}} \frac{\mathrm{dE}_{0\mathrm{p,s}}}{\mathrm{dz}} - k_{\mathrm{p,s}}^2 \mathrm{E}_{0\mathrm{p,s}} \right) e^{i(\omega_{\mathrm{p,S}} t \mp k_{\mathrm{p,S}} z)} + c.c. \tag{2.67}$$

where the minus and plus signs apply with E_{0p} and E_{0s} respectively. Using Eqs. (2.60), (2.61), and (2.67), the wave equation (2.50) is separated into two equations at the frequencies ω_p and ω_s as the following:

$$-ik_{\mathrm{p}} \frac{\mathrm{dE}_{0\mathrm{P}}}{\mathrm{dz}} e^{i(\omega_{\mathrm{p}} t - k_{\mathrm{p}} z)} + c.c. = \mu_0 \frac{\partial^2 \mathrm{P}_{\mathrm{NL}}^{\omega_{\mathrm{p}}}}{\partial t^2} \tag{2.68}$$

$$ik_{S} \frac{\mathrm{dE}_{0\mathrm{S}}}{\mathrm{dz}} e^{i(\omega_{\mathrm{S}} t + k_{S} z)} + c.c. = \mu_0 \frac{\partial^2 \mathrm{P}_{\mathrm{NL}}^{\omega_{\mathrm{S}}}}{\partial t^2} \tag{2.69}$$

where $\mathrm{P}_{\mathrm{NL}}^{\omega_{\mathrm{p}}}$ and $\mathrm{P}_{\mathrm{NL}}^{\omega_{\mathrm{S}}}$, the nonlinear polarizations oscillating at ω_p and ω_s, are given by:

$$\mathrm{P}_{\mathrm{NL}}^{\omega_{\mathrm{p}}} = \frac{\gamma_e}{\rho_0} \rho \mathrm{E}_{\mathrm{S}} = \frac{\gamma_e}{4\rho_0} [\mathrm{AE}_{0\mathrm{s}} e^{i(\omega_{\mathrm{p}} t - k_{\mathrm{p}} z)} + c.c.] \tag{2.70}$$

$$\mathrm{P}_{\mathrm{NL}}^{\omega_{\mathrm{S}}} = \frac{\gamma_e}{\rho_0} \rho \mathrm{E}_{\mathrm{P}} = \frac{\gamma_e}{4\rho_0} [\mathrm{AE}_{0\mathrm{P}}^{*} e^{-i(\omega_{\mathrm{S}} t + k_{\mathrm{S}} z)} + c.c.] \tag{2.71}$$

By substituting Eqs. (2.70) and (2.71) into Eqs. (2.68) and (2.69) respectively, the following equations will result:

$$\frac{\mathrm{dE}_{0\mathrm{p}}}{\mathrm{dz}} = -K\left|E_{0\mathrm{s}}\right|^2 \mathrm{E}_{0\mathrm{p}} \tag{2.72}$$

$$\frac{\mathrm{dE}_{0\mathrm{s}}}{\mathrm{dz}} = -K\left|E_{0\mathrm{p}}\right|^2 \mathrm{E}_{0\mathrm{s}} \tag{2.73}$$

in which K is given by

$$K = \frac{-i\mu_0\omega_{\mathrm{p}}\gamma_e^2/8\rho_0\mathrm{v}_{\mathrm{a}}}{(\omega_{\mathrm{p}}-\omega_s)-\omega_{\mathrm{a}}+i\Gamma_{\mathrm{B}}} \tag{2.74}$$

with the assumption $\mathrm{v}_{\mathrm{p}} \approx \mathrm{v}_s \approx c/n$, $k_{\mathrm{a}} = 2k_{\mathrm{p}}$ obtained from Eq. (2.54) in backward scattering ($\gamma = \pi$), $\Gamma_B = \Gamma k_{\mathrm{a}}^2/2$ and $\omega_{\mathrm{p}} - \omega_s \approx \omega_{\mathrm{a}} = k_{\mathrm{a}}\mathrm{v}_{\mathrm{a}} = 2\omega_{\mathrm{p}} n\mathrm{v}_{\mathrm{a}}/c$. By adding the effect of absorption using the absorption coefficients α_{p} and α_s for pump and Stokes waves respectively, the following equations can be obtained:

$$\frac{\mathrm{dI}_{\mathrm{p}}}{\mathrm{dz}} = -g_B\mathrm{I}_{\mathrm{p}}\mathrm{I}_s - \alpha_{\mathrm{p}}\mathrm{I}_{\mathrm{p}} \tag{2.75}$$

$$\frac{\mathrm{dI}_s}{\mathrm{dz}} = -g_B\mathrm{I}_{\mathrm{p}}\mathrm{I}_s + \alpha_s\mathrm{I}_s \tag{2.76}$$

where g_B, known as the Brillouin gain factor is:

$$g_B = g_B^{(0)}\left(\frac{\Gamma_B^2}{(\omega_{\mathrm{a}}-(\omega_{\mathrm{p}}-\omega_s))^2+\Gamma_B^2}\right) \tag{2.77}$$

The maximum Brillouin gain factor given by $g_B^{(0)} = \dfrac{\omega_{\mathrm{p}}^2\gamma_e^2}{4\rho_0\varepsilon_0\mathrm{v}_{\mathrm{a}}c^2\Gamma_B}$ at resonance $(\Delta\omega = \omega_{\mathrm{a}} - (\omega_{\mathrm{p}} - \omega_s) = 0)$ is independent of the incident light frequency ω_{p}. However, ω_{a} the frequency of acoustic wave and Γ_B, the line width of the Brillouin gain depend on the light frequency ω_{p} since we can deduce from Eq. (2.54) that

$$\omega_a = k_a v_a = \frac{2nv_a\omega_p}{c}\sin\gamma/2 \tag{2.78}$$

$$\Gamma_B = k_a^2\Gamma/2 = \frac{2\Gamma n^2\omega_p^2}{c^2}\sin^2\gamma/2 \tag{2.79}$$

As mentioned before, Brillouin scattering can not propagate in the same direction as the pump because according to Eq. (2.79) the damping coefficient $\Gamma_B = 0$ when $\gamma = 0$, i.e. $\mathbf{k}_p$ and $\mathbf{k}_s$ are parallel. In addition, the density function ρ induced by the field can not be in the form of Eq. (2.62) when $\Gamma_B = 0$. In addition, Eq. (2.79) also suggests that Γ_B has its largest possible value as $\gamma = \pi$ or $\mathbf{k}_p = -\mathbf{k}_s$ so that the medium of Brillouin cell forms a scattering grating derived by Eq. (2.62) as the respond to the electric fields. It is evident that g_B will be reduced to one-half of its peak value $g_B^{(0)}$ when $\Delta\omega = \pm\Gamma_B$ so that the Brillouin gain spectrum width $\Delta\omega_B$ is defined as the full width at half maximum (FWHM) of the Brillouin gain function g_B and it is equal to $2\Gamma_B$ ($\Delta\omega_B = 2\Gamma_B$). The Brillouin gain linewidth is generally different for various optical fibers since inhomogeneities in the fiber core cross sections along the fiber length vary for different fibers. In optical fibers, $\Delta\nu_B = \Delta\omega_B/2\pi$ is typically between 10 and 100 MHz in the 1550 nm spectral region whereas the measured Brillouin shift, $\Omega_B = \omega_B/2\pi$, is about 11GHz [31].

In Eqs. (2.75) and (2.76), it is assumed that the counterpropagating pump and Stokes waves are linearly polarized and maintain their polarization along the fiber. In practice, this assumption is true when the fiber is a polarization-maintaining fiber and the pump and Stokes waves are polarized along its principal axis. In a conventional optical fiber such as a SMF however, the relative

polarization angle between the pump and Stokes wave varies randomly as discussed in section 2.3.2. This is the case that the Brillouin gain factor g_B will be reduced by a prefactor of 1.5 [35]. Analytical solutions of the coupled intensity in Eqs. (2.75) and (2.76) can be derived as the following.

In order to solve the coupled steady state of Eqs. (2.75) and (2.76) describing the SBS dynamics in a SMF, the following transformation can be introduced by these definitions [36]

$$\Sigma = I_p - I_s \quad , \quad \Delta = I_p + I_s \tag{2.80}$$

so that

$$I_p I_s = \frac{1}{4}(\Delta^2 - \Sigma^2) \tag{2.81}$$

Subtracting Eq. (2.75) from Eq. (2.76) results in

$$\frac{d\Sigma}{dz} = -\alpha\Delta \tag{2.82}$$

On the other hand, adding Eqs. (2.75) and (2.76) and using Eq. (2.81) gives

$$\frac{d\Delta}{dz} = -\alpha\Sigma - \frac{g_B}{2}(\Delta^2 - \Sigma^2) \tag{2.83}$$

If Δ is multiplied to both sides of the last equation, by using Eq. (2.82) it is obtained

$$\frac{d}{dz}(\Delta^2 - \Sigma^2) = \frac{g_B}{\alpha}(\Delta^2 - \Sigma^2)\frac{d\Sigma}{dz} \tag{2.84}$$

By integrating the last equation over the fiber length from $z = 0$ to a given point, a conservation relation will be obtained as

$$\mathrm{Ln}(\Delta^2 - \Sigma^2) - \frac{g_B}{\alpha}\Sigma = \left\{\mathrm{Ln}(\Delta^2 - \Sigma^2) - \frac{g_B}{\alpha}\Sigma\right\}_{z=0} = \text{constant} \tag{2.85}$$

Therefore, Δ can be obtained in terms of Σ by getting the exponential function from Eq. (2.84) as

$$\Delta = \sqrt{(\Delta_0^2 - \Sigma_0^2)\exp[\frac{g_B}{\alpha}(\Sigma - \Sigma_0)] + \Sigma^2} \tag{2.86}$$

where $\Sigma_0 = \Sigma(z=0)$ and $\Delta_0 = \Delta(z=0)$. From Eqs. (2.82) and (2.85), it is revealed that Σ can be solved exactly by using the following integration

$$\int_{\Sigma_0}^{\Sigma(z)} \frac{\mathrm{dx}}{\sqrt{(\Delta_0^2 - \Sigma_0^2)\exp[\frac{g_B}{\alpha}(x - \Sigma_0)] + x^2}} = -\alpha z \tag{2.87}$$

However, no closed form solution has been found for this integral. The last two equations are applicable for all values of g_B and α except for the case of zero attenuation (α=0). For this case, the following result can be obtained readily by integrating Eq. (2.82) as

$$\mathrm{I_p} - \mathrm{I_s} = \mathrm{I_{p_o}} - \mathrm{I_{s_0}} = k' = \text{constant} \tag{2.88}$$

which is a conservation law for energy with the assumption $\mathrm{I_{p_0}} = \mathrm{I_p}(z=0)$ and $\mathrm{I_{s_0}} = \mathrm{I_s}(z=0)$. This solution shows that the difference of intensity of the pump and Stokes waves remains constant through the medium at least for the lossless fiber approximation. In addition, Eqs. (2.75) and (2.76) for this case can be solved exactly to yield

$$\mathrm{I_p}(z) = \frac{\frac{\mathrm{I_{p_0}}}{\mathrm{I_{s_0}}} - 1}{\frac{\mathrm{I_{p_0}}}{\mathrm{I_{s_0}}} - \exp(-g_B k' z)} \mathrm{I_{p_0}} \tag{2.89}$$

$$\mathrm{I_s}(z) = \frac{1 - \frac{\mathrm{I_{s_0}}}{\mathrm{I_{p_0}}}}{\exp(\mathrm{g_B} k' z) - \frac{\mathrm{I_{s_0}}}{\mathrm{I_{p_0}}}} \mathrm{I_{s_0}} \tag{2.90}$$

where k' is a constant according to Eq. (2.85). Therefore, it can be deduced from the last two equations that in a lossless fiber approximation the pump and Stokes intensity are related together by

$$I_s(z) = I_p(z)\frac{I_{s_0}}{I_{p_0}}\exp(-g_B k' z) \tag{2.91}$$

In the other approximation called the no depletion pump, the pump intensity I_p is constant. Due to the relatively small values of the acoustic wave frequency ω_a, we have $\omega_p \approx \omega_s$ and so $\alpha_p \approx \alpha_s \equiv \alpha$. When there is a weak nonlinear coupling, so that $I_s << I_p$, the solutions of the coupled Eqs. (2.75) and (2.76)

$$I_p(z) = I_p(0)\exp(-\alpha\ z) \tag{2.92}$$

$$I_s(z) = I_s(L)\exp(\alpha(z-L))\exp(g_B I_p(0)[\exp(-\alpha z) - \exp(-\alpha L)]/\alpha) \tag{2.93}$$

where the integration in Eq. (2.93) is done from the whole fiber length L to the given point z due to the backward propagation nature of the Stokes wave. In practice, a given Stokes input at $z = L$ will grow to produce an output intensity at $z = 0$ as

$$I_s(0) = I_s(L)\exp[(g_B P_0 L_{eff.}/A_{eff.}) - \alpha L)] \tag{2.94}$$

with the assumption $P_0 = I_p(0)A_{eff.}$ is the input pump power, $A_{eff.} = \pi w$ is the effective core area of the Stokes wave in an optical fiber where w is the spot size of the beam, and $L_{eff.}$ is the effective interaction length obtained by

$$L_{eff.} = \frac{1}{\alpha}[1 - \exp(-\alpha L)] \tag{2.95}$$

The effective interaction length, L_{eff}, is smaller than the actual fiber length L due to fiber loss. For a long fiber, such as our case in where we use a 25 km SMF, $\exp(-\alpha L) << 1$, so that

$$L_{\text{eff}} \approx 1/\alpha \approx 22.86 \ \text{(km)} \tag{2.96}$$

where $\alpha = 0.19$ (dB/km) = 0.0437 $(\text{km})^{-1}$. In both approximations, Eqs. (2.90) and (2.93) describe an increase in Stokes intensity I_s when it propagates because the Brillouin-scattered Stokes field is supposed to propagate in the –z direction. Therefore, the discussed phenomenon is a stimulated Brillouin scattering (SBS) process in which the Backward Brillouin scattering originates usually from noise or spontaneous Brillouin scattering occurring through the fiber. However, in a Brillouin fiber laser, a Stokes wave incident at $z = L$ is generally fed as a positive feedback which will be discussed later. It is clear that the approximation of undepleted pump breaks when I_s becomes comparable in magnitude to the pump intensity I_p.

One of the important features of the Brillouin scattering process is the SBS threshold defined theoretically as the input pump intensity at which the resonant gain for Brillouin Stokes wave, $g_B(\Delta\omega = 0)$, is equal to its loss over the same given distance. By setting $\frac{dI_s}{dz} = 0$ in Eq. (2.76), the pump intensity at threshold is found to be

$$I_{p_{th}} = \frac{\alpha}{g_B^{(0)}} = \frac{4\alpha\rho_0\varepsilon_0 v_a \Gamma_B}{\omega_p^2 \gamma_e^2} \tag{2.97}$$

For a free end optical fiber in which Brillouin Stokes wave grows only from spontaneous Brillouin scattering throughout the fiber, the Brillouin threshold is found analytically to occur at a threshold pump power P_{th} at which the backscattered Stokes power is equal to the input pump power [37]:

$$P_{th} \approx 21\frac{A_{\text{eff}}}{g_B^{(0)} L_{\text{eff}}} \tag{2.98}$$

In optical communication systems at 1550nm, the typical values for optical fibers are $A_{eff} = 50\mu m^2$, $L_{eff} \approx 21km$, and $g_B^{(0)} = 5\times10^{-11}\,m/W$, Eq. (2.94) results in $P_{th} \approx 1mW$. However, the backscattered Stokes power is always less than the input power due to pump depletion in practice. In the other study, it is shown that the threshold power defined by Eq. (2.98) is the pump power required to produce an SBS output power at the level of Rayleigh back scattering power [38]. Again, it is revealed that $g_B^{(0)}$ is nearly independent of the pump frequency ω_p since $\Gamma_B \propto \omega_p^2$ according to Eq. (2.79). Besides, the Brillouin gain in Eq. (2.77) is obtained under steady state conditions for a continuous pump wave whose spectral width $\Delta\nu_p$ is much smaller than the Brillouin gain $\Delta\nu_B$. However, the Brillouin gain will be reduced considerably if the spectral width of the pump wave exceeds the Brillouin gain spectral width ($\Delta\nu_p > \Delta\nu_B$). If the Brillouin pump laser has a Lorentzian spectral profile, it can be shown that the Brillouin gain spectrum $g_B(\omega)$ is still given by Eq. (2.77) but the gain peak $g_B^{(0)}$ is reduced by a factor $[1+(\Delta\nu_p/\Delta\nu_B)]$ [39]. Therefore, in this case, the SBS threshold increases by the factor $1+(\Delta\nu_p/\Delta\nu_B)$ so that

$$P_{th} \approx 21\frac{A_{eff}}{g_B^{(0)}L_{eff}}\left(1+\frac{\Delta\nu_p}{\Delta\nu_B}\right) \tag{2.99}$$

It should be mentioned that single-mode optical fibers behave as highly multimode acoustic waveguides having finite numerical apertures. Therefore, an optical beam can be scattered at a non-zero angle from the fiber axis and at the same time, can remain fully guided if the angle is small enough. This small- angle effect causes acoustic waves to propagate radially on the fiber's cladding and such acoustic waves are known as transverse waves that generate cladding Brillouin

scattering (CBS). This is referred to as the electrostriction mechanism or the acoustic interaction in optical telecommunications [40],[41], or as spontaneous guided-acoustic-wave Brillouin scattering in quantum optics [42]. CBS-induced passive mode-locking of fiber lasers has also been reported [43],[44]. Low-frequency CBS-scattered satellites of the Brillouin signal result in new dynamical features of SBS such as Brillouin fiber lasers which will be discussed in the next section [45].

2.6 Brillouin Fiber Laser (BFL) Generation

If an optical fiber is placed inside a cavity, Brillouin fiber lasers (BFLs) can be generated by using the Brillouin gain function g_B in the fiber. BFLs have been an active topic of research since 1976 [46],[47],[48]. Using optical circulators and optical couplers, there is no need to use mirrors for BFL generation in fiber optics. The SBS threshold power can be considerably reduced by placing an optical fiber in a cavity to generate BFL oscillations. In addition, the Brillouin Stokes linewidth becomes significantly narrower than the pump linewidth with reductions of up to a few Hertz [49],[50]. For a conventional ring cavity shown in Fig. 2.4 , the boundary condition for the Brillouin Stokes intensity is

$$\mathrm{I}_s(L) = R \times \mathrm{I}_s(0) \tag{2.100}$$

where L is the ring-cavity length and R is equal to the fraction of the Brillouin Stokes intensity injected into the ring cavity after each round trip.

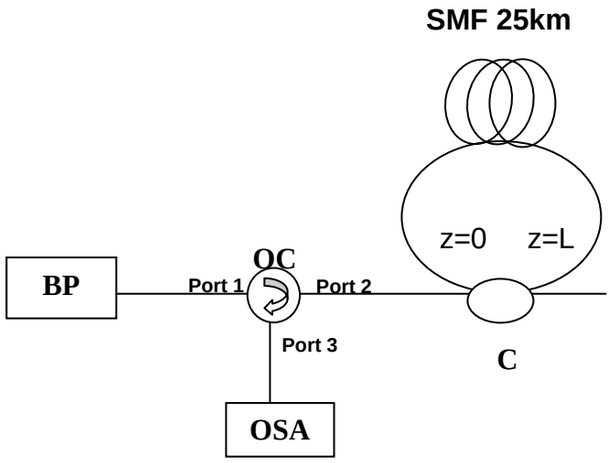

Fig. 2.1: A conventional ring cavity for BFL generation

It is evident that the Brillouin Stokes wave is generated in the backward direction due to spontaneous Brillouin scattering at the beginning, however, after generating BFL oscillations, we can ignore the spontaneous Brillouin Stokes intensity in comparison to the feedback Stokes. Therefore, the coupled intensity equations for the ring cavity BFL have the forms:

$$\frac{dI_p}{dz} = -g_B I_p I_s - \alpha_p I_p \tag{2.101}$$

$$\frac{dI_s}{dz} = -g_B I_p I_s + \alpha_s I_s \tag{2.102}$$

where the parameters are the same as in Eqs. (2.75) and (2.76). In addition to Eq. (2.100), there is another boundary condition for the intensity pump power in the fiber:

$$I_p(z=0) = I_0\mu + R \times I_p(z=L) \tag{2.103}$$

I_0 is the pump intensity injected into the optical system and μ plays the role of a dimensionless pump factor. In this case, using the boundary condition in Eq. (2.100), the SBS threshold condition for the undepleted pump approximation will be:

$$R \times \exp(g_B \mathrm{P_{th}} L_{eff} / \mathrm{A_{eff}} - \alpha L) = 1 \qquad (2.104)$$

Fabry-Perot Brillouin fiber lasers have some aspects that make it qualitatively different from those making use of a ring cavity. This difference is due to the simultaneous attending of the forward and backward propagating components of the Brillouin pump and Stokes in the cavity. Therefore, higher order Stokes waves generated through cascading SBS are readily performed in the linear cavity than in the ring one with the same conditions. In the process of cascading SBS, each Stokes components pumps the next order Stokes component after its power becomes large enough to satisfy the condition of Brillouin threshold power. At the same time, anti-Stokes waves are also generated through another physical process called four-wave mixing between copropagating pump and Stokes waves.

2.7 General Characteristics

Optical sources such as fiber lasers can be evaluated based on a number of characteristics which are briefly introduced here as the basis of most of the theoretical and experimental works that are carried out in the subsequent chapters. These characteristics include output power, operational wavelength, spectral linewidth and threshold power will be discussed in what is to follow.

2.7.1 Output Power

The most important characteristic of an optical source especially in nonlinear optics is its output power. In both linear and nonlinear optics, it is useful to express received power I (and also the transmitted power for all components) in decibel units defined as

$$\mathrm{I\ (in\ dBm)} = 10\ \mathrm{Log_{10}\ I\ (in\ mW)} \qquad (2.105)$$

The letter m in dBm is a reminder of the reference level of 1 mW chosen for convenience. In this decibel scale for the absolute power, 1 mW corresponds to 0 dBm, whereas powers less than 1 mW are expressed as negative numbers. The amount of power required depends on the applications. In fiber optics communications for example, the launched power is normally less than a few miliwatts due to SBS generation [51] whereas large powers are used commonly in experiments on nonlinear fiber optics. Higher power optical sources are now available at reasonable prices; however, the maximum optical power is limited by a few factors, such as nonlinear phenomena (scattering especially SBS as cited before), the damage threshold of the components and the safety of the users. The damage threshold power of components must be considered particularly when amplifiers are used. For example, damage to the connector's ferrule has been reported to occur at a source power of about 16 dBm [52].

2.7.2 Operational Wavelength

At the time of writing, the 1550 nm wavelength is the most widely used wavelength since the minimum loss of single-mode fibers is about 0.2 dB/km near 1550 nm as shown in Fig 1.1. The advantage of using a single-mode optical fiber is that this type of fiber has less internal (Rayleigh) scattering in comparison to multimode optical fibers. A secondary minimum less than 0.35 dB/km occurs near the 1310nm wavelength region. Note that the peak near 1.4 μm and a smaller peak near 1.23 μm seen in Figure 1.1 occur due to absorption caused by hydroxyl (OH) impurities or residual water vapour in the silica fiber [51]. Therefore, it is only logical that the operational wavelength of most commercial optical components and also optical sources to be near 1550 nm. However, in special works such as

Erbium and Ytterbium optical amplifiers where we have to use other wavelengths of 980 nm and 1060 nm respectively, optical sources and optical components suitable in these regions of operational wavelengths should be made available.

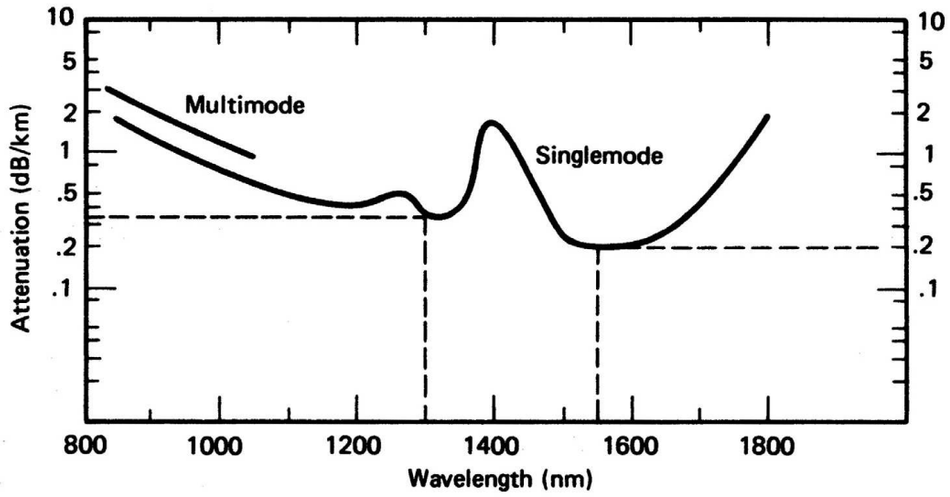

Fig. 2.2: Fiber attenuation as a function of wavelength for standard single-mode optical fiber.

2.7.3 Linewidth

Linewidth is defined as the full width at half maximum (FWHM) of a power spectrum. In the decibel scale, it is equal to the width of the spectrum at -3 dB of the maximum power. In nonlinear optics, SBS threshold power depends on the linewidth or spectral width of the source or pump power; in other words, the SBS threshold increases when the spectral width of the pump power increases with the condition that the spectral width of the pump is much greater than the spectral width of the Brillouin gain spectrum [53]. In optical fiber communication systems, the smaller the spectral width, the better the condition for communication; however, this requirement is reversed in sensor systems. That's to say, a smaller spectral width source contributes to a smaller material dispersion in a silica fiber optics, so that a broader bandwidth is allowed in optical communication [54]. In

contrast, the smaller spectral width in a sensor system contributes to a higher coherent noise [55]. The coherent noise is not a factor in optical communication because the transmission distance is long enough that the coherency noise is lost. In chapter 4, we discuss the method used in this work to measure the ultra-narrow BFL linewidth which is reported from to be in the range of a few Hz to a few kHz.

2.7.4 Threshold Power

The minimum amount of pump power required for a laser source to begin lasing is defined as the threshold power. When the pump power is below the threshold power, the output power of the laser source is incoherent and spontaneous. Pumping above the threshold results in a narrowing of the spectral width. Lower lasing threshold is preferred for a laser source since lower optical pump power consumption is required. In an optical transmission system, however, to increase the transmission distance by using a high-input power requires the SBS threshold to be increased. In a cavity, a low threshold power requires low cavity losses and high gain efficiency. The question of what values are most appropriate for the threshold pump power is one of the fundamental issues of laser design. The threshold can be characterized by three phenomena; the sudden increment in power, the significant reduction in the spectral width, and the clamping of the amplified spontaneous emission (ASE) level.

References

[1] Y. R. Shen, *The Principle of Nonlinear Optics*, Wiley, New York, 1984.

[2] T. Okoshia, *Optical Fibers*, Academic Press, New York, 1982.

[3] D. Gloge, " Weakly Guiding Fibers," Applied Optics vol. 10, pp. 2252-2258, 1971.

[4] W. B. Jones, *Introduction to Optical Fiber Communication System*, Holt, Rinehart, and Winston, New York, 1988.

[5] J. Gower, *Optical Communication System,* 2nd ed., Prentice Hall, London, 1993.

[6] A. W. Snyder and J. D. Love, *Optical Waveguide Theory,* Chapman and Hall, 1983.

[7] L. B. Jeunhomme, *Single-Mode Fiber Optics*, Marcel Dekker, New York, 1990.

[8] D. Marcuse, "Loss Analysis of Single-Mode Fiber Splices," Bell System Technical J. vol. 56, pp. 703-718, 1977.

[9] D. Marcuse, "Gaussian approximation of the fundamental modes of graded-index fibers," J. Opt. Soc. Am. vol. 68, pp. 103-109, 1978.

[10] A. W. Snyder and R. A. Sammut, "Fundamental (HE_{11}) Modes of Graded Optical Fiber," J. Opt. Soc. Am., vol. 69, pp. 1663-1671, 1980.

[11] R. B. Dyott, *Elliptical Fiber Waveguides,* Artec House, Boston, 1995.

[12] T. Li (ed.), *Optical Fiber Communication: Fiber Fabrication*, Vol. 1, Academic Press, San Diego, 1985.

[13] B. J. Ainslie and C. R. Day, "A review of single-mode fibers with modified dispersion characteristics," J. Lightwave Technol. 4, pp. 967–979, 1986.

[14] A. H. Gnauck and R. M. Jopson, *Optical Fiber Telecommunication III*, I. P. Kaminow and T. L. Koch, eds., Academic Press, San Diego, CA, 1997.

[15] C. D. Poole, J. M. Wiesenfeld, and A. R. McCormick, and K. T. Nelson, "Broadband dispersion compensation by using the higher-order spatial mode in a two-mode fiber," Opt. Lett. vol. 17, pp. 985-987, 1992.

[16] A. M. Vengsarkar and W. A. Reed, “Dispersion-compensating single-mode fibers: efficient designs for first- and second-order compensation,” Opt. Lett. vol. 18, pp. 924-926, 1993.

[17] C. D. Poole, J. M. Wiesenfeld and D. J. Digiovanni, “Elliptical-core dual-mode fiber dispersion compensator,” IEEE Photonics Technology Letters vol. 5, pp.194 – 197, 1993.

[18] C. D. Poole, J. M. Wiesenfeld and D. J. Digiovanni, and A. M. Vengsarkar, “Optical fiber-based dispersion compensation using higher order modes near cutoff,” J. Lightwave Technol. 12, pp. 1746-1758, 1994.

[19] J. E. Midwinter, *Optical Fiber for Transmission,* Chichester John Wiley & Sons, New York, 1979.

[20] F. Urbach, “The long-wavelength edge of photographic sensitivity and of the electronic absorption of solids,” Physical Review vol. 92, pp. 1324-1324 ,1953.

[21] S. R. Nagel, J. B. MacChesney, and K. L. Walker, “An overview of the modified chemical vapor deposition (MCVD) process and performance,” IEEE Journal of Quantum Electronics vol. 18, pp. 459-476, 1982.

[22] T. Li (ed.), *Optical Fiber Communications: Fiber Fabrication*, Vol. 1, Academic Press, San Diego, 1985.

[23] T. Miya, Y. Terunuma, T. Hosaka, and T. Miyoshita, “Ultimate low-loss single-mode fiber at 1.55 μm,” pp. 106-108, 1979.

[24] G. A. Thomas, B. L. Shraiman, P. F. Glodis, and M. J. Stephan, “Toward the clarity limit in optical fiber,” Nature vol.404, pp. 262-264, 2000.

[25] P. K. Cheo, *Fiber Optics, Devices and Systems,* Prentice-Hall, Englewood Cliffs, New Jersey, 1985.

[26] J. D. Jackson, Classical Electrodynamics, 2 nd. ed., John Wiley & Sons, New York, 1975.

[27] M. E. Lines, “The search for very low loss fiber optic materials,” Science vol.226, pp. 663-668, 1984.

[28] K. Tsujikawa, and M. Ohashi, “Rayleigh scattering in K_2O-MgO- Si_2O and Na_2O- B_2O_3 - Si_2O glass,” Optical Fiber Thechnology vol.6, pp. 74-82, 2000.

[29] M. F. Churbanov, “High purity chalcogenide glasses as material for fiber optics,” J. Non-Cryst. Solids vol. 184, pp. 25-29, 1995.

[30] D. Marcuse, *Light Transmission Optics*, Van Nostrand Reinhold Series, New York, 1989.

[31] G. P. Agrawal, *Nonlinear Fiber Optics*, 3 rd ed., Academic, New York, 2001.

[32] I. L. Fabelinskii, *Molecular Scattering of Light*, Plenum Press, New York, 1968, p. 506.

[33] A. Kobyakov, S. Kumar, D. Q. Chowdhury, A. B. Ruffin, M. Sauer, S. R. Bickham, and R. Mishra, “Design concept for optical fibers with enhanced SBS threshold,” Opt. Express vol. 13, pp. 5338-5347, 2005.

[34] R. W. Boyd, *Nonlinear Optics*, Academic Press, San Diego, CA, 1992.

[35] M. O. van Deventer and A. J. Boot, “Polarization properties of stimulated Brillouin scattering in single-mode fibers,” J. Lightwave Technol. vol. 12, pp. 585-590, 1994.

[36] L. Chen and X. Bao, “Analytical and numerical solutions for steady state stimulated Brillouin scattering in a single-mode fiber,” Optics Communications vol. 152, pp. 65-70, 1998.

[37] R. G. Smith, “Optical power handling capacity of low loss optical fibers as determined by stimulated Raman and Brillouin scattering,” Applied Optics vol. 11, pp. 2489- 2494, 1972.

[38] X. P. Mao, R. W. Tkach, A. R. Chraplyvy, R. M. Jopson, and R. M. Derosier, “Stimulated Brillouin threshold dependence on fiber type and uniformity,” IEEE Photon. Technol. Lett. vol. 4, pp. 66-68, 1992.

[39] E. Lichtman, A. A. Friesem, R. G. Waarts, and H. H. Yaffe, “Stimulated Brillouin scattering excited by two pump waves in single-mode fibers,” J. Opt. Soc. Am. B vol. 4, 1397-1403, 1987.

[40] E. M. Dianov, A. V. Luchnikov, A. N. Pilipetskii, A. N. Starodumov, “Electrostriction mechanism of soliton interaction in optical fibers,”Opt. Lett. vol. 15, pp. 314-316, 1990.

[41] I. Bongrand, A. Picozzi, E. Picholle, “Coherent model of cladding Brillouin scattering in single mode fibres ,” Electron. Lett. vol. 34, pp. 1769-1770, 1998.

[42] R. M. Shelby, M. D. Levenson, P. W. Bayer, “Guided acoustic-wave Brillouin scattering,” Phys. Rev. B vol.31, pp.5244-5252,1985.

[43] A. B. Grunidin, D. J. Richardson, D. N. Payne, “Passive harmonic. modelocking of a fiber soliton ring laser ,”Electron. Lett. vol. 29, pp. 1860-1861 ,1993.

[44] A. N. Pilipetskii, E. A. Golovchenko, C. R. Menyuk, **“**Acoustic effect in passively mode-locked fiber ring lasers ” Opt. Lett. vol. 20, pp. 907-909, 1995.

[45] I. Bongrand, C. Montes, E. Picholle, J. Botineau, A. Picozzi, C. Cheval, D. Bahloul, “Soliton compression in a Brillouin fiber ring laser,” Opt. Lett. vol. 26, pp. 1475-1477, 2001.

[46] K. O. Hill**,** B. S. Kawasaki**,** and D. C. Johnson, “cw Brillouin laser,” Appl. Phys. Lett. vol. 28, p. 608-609, 1976**.**

[47] C. Montes, D. Bahloul, I. Bongrand, J. Botineau, G. Cheval, A. Mahmhoud, E. Picholle, and A. Picozzi, “Self-pulsing and dynamic bistability in cw-pumped Brillouin fiber ring lasers,” J. Opt. Soc. Am. B vol. 16, pp. 932-951, 1999.

[48] M. R. Shirazi, S. W. Harun, M. Biglari, H. Ahmad, “Linear cavity Brillouin fiber laser with improved characteristics,” OPTICS LETTERS vol. 33, pp.770-772, 2008.

[49] S. P. Smith, F. Zarinetchi, and S. Ezekiel, “ Narrow-linewidth stimulated Brillouin fiber laser and applications,” *Opt. Lett.*, vol. 16, pp. 393–395, 1991.

[50] M. R. Shirazi, S. W. Harun, M. Biglary, K. Thambiratnam, and H. Ahmad, “Effect of Brillouin pump linewidth on the performance of Brillouin Fiber Lasers,” ISAST Transactions on Electronics and Signal Processing, No. 1, vol. 1, pp. 30-32, 2007.

[51] G. P. Agrawal, *Fiber-Optics Communication Systems*, 3rd ed., Academic, New York, 2002.

[52] B. E. A. Saleh, and M. C. Teich, Fundamentals of Photonics, John Wiley, New York, 1991.

[53] G. P. Agrawal, *Nonlinear Fiber Optics*, 3 rd ed., Academic, New York, 2001.

[54] J. C. Palais, *Fiber Optic Communication, 5th* ed., Prentice Hall, 2002.

[55] P. F. Wysocki, “Characteristics of Erbium-doped superfluorescent fiber source for interferometric sensor application,” J. Lightwave Technol. vol. 12, pp. 550-567, 1994.